

# Fast Online Planning for Bipedal Locomotion via Centroidal Model Predictive Gait Synthesis

Yijie Guo<sup>1</sup>, Mingguo Zhao<sup>2</sup>

**Abstract**—The planning of whole-body motion and step time for bipedal locomotion is constructed as a model predictive control (MPC) problem, in which a sequence of optimization problems need to be solved online. While directly solving these optimization problems is extremely time-consuming, we propose a predictive gait synthesizer to solve them quickly online. Based on the full dimensional model, a library of gaits with different speeds and periods is first constructed offline. Then the proposed gait synthesizer generates real-time gaits by synthesizing the gait library based on online prediction of centroidal dynamics. We prove that the generated gaits are feasible solutions of the MPC optimization problems. Thus our proposed gait synthesizer works as a fast MPC-style planner to guarantee the stability of robots. Simulation and experimental results on an 8 degrees of freedom (DoF) bipedal robot are provided to show the performance and robustness of this method for walking and standing.

## I. INTRODUCTION

Bipedal robots are complex dynamic systems with high degrees of freedom. Different methods have been investigated for real-time motion planning for bipedal robots. Classical methods based on reduced-order models have been well developed[1], [2], [3], while the workspace of robots may be limited and some physical constraints (actuator bounds, friction cone, etc.) are not directly considered. Thus, a lot of recent work [4], [5] focused on trajectory optimization based on full dimensional models. However, due to the complexity and non-convexity of the formulated nonlinear optimization problems, these methods are not yet ready for online implementation.

In order to consider full dimensional dynamics/constraints and avoid online trajectory optimization, gait library based methods have been proposed. Through trajectory optimization based on full dimensional models, these methods first construct a library of periodic or aperiodic gait trajectories offline, then choose appropriate trajectories online. One of the earliest work based on this idea is [6], where gaits with fixed speeds are designed for a planar underactuated biped. This idea was later extended to fully-actuated bipedal robots in [7], [8]. In these studies, gait trajectories are chosen according to the speed command. For these command-based gait library methods, the stability of the robot heavily relies on the controller, since the motion planning does not change according to robot states. Under large disturbance, these methods may fail when the controller can not track the planned motion due to physical constraints of actuators or

<sup>1</sup>Yijie Guo is with Beijing Institute of UBTECH Robotics, Beijing, China. fugo.guo@ubtrobot.com

<sup>2</sup>Mingguo Zhao is with the Department of Automation, Tsinghua University, Beijing, China mgzhao@mail.tsinghua.edu.cn

ground reaction force. To address this issue, a gait updating method is proposed in [9], by updating gait trajectories according to the mid-step average speed, robots can handle larger speed perturbation. However, as the gait is updated only once at the middle of each step, it can not react in time for large disturbance near the beginning or end of each step.

In the meantime, current gait library methods generally keep a constant step time, while adjusting both step location and step time greatly enlarges the margin of stability, as shown in [10]. In related work [11], [12] on motion planning based on reduced-order models, step time adjustment has also been applied to improve the robustness of robots. It is shown in [13] that the area of capturability region increases as the minimum step time decreases, while walking consistently with a very short step time is unnatural and power-consuming, and users may require a specific step time in some cases. This brings the need for online step time adjustment to meet the user command under normal condition and satisfy the stability requirement under disturbances.

To address above two issues, we propose a gait synthesis method from an MPC point of view. The proposed gait synthesizer generates real-time gaits by synthesizing a multi-period gait library based on online prediction of centroidal dynamics. This enables fast reactive gait updating at each time instant. Furthermore, step time is adjusted online by synthesizing gaits with different periods. With this proposed method, robots can achieve flexible transitions between standing and walking with different periods/speeds according to the user command and robust locomotion under large disturbances and environmental uncertainties.

The paper is organized as follows. The MPC problem for locomotion planning is described in Sec. II. Then the multi-period gait library is constructed in Sec. III. In Sec. IV, the predictive gait synthesizer is proposed and proved to offer feasible solutions for the MPC optimization problems. Finally, simulation and experimental results on an 8-DoF bipedal robot are presented in Sec. V.

## II. PROBLEM DESCRIPTION

The overall motion planning and control architecture is shown in Fig. 1. The planner generates whole-body motion trajectories according to the user command and current robot states, then an operational space controller (OSC) generates appropriate motor commands to follow these trajectories. We focus on the motion planning part in this paper.

Our proposed gait synthesizer is an MPC style planner, the basic idea is to solve the following optimization problem

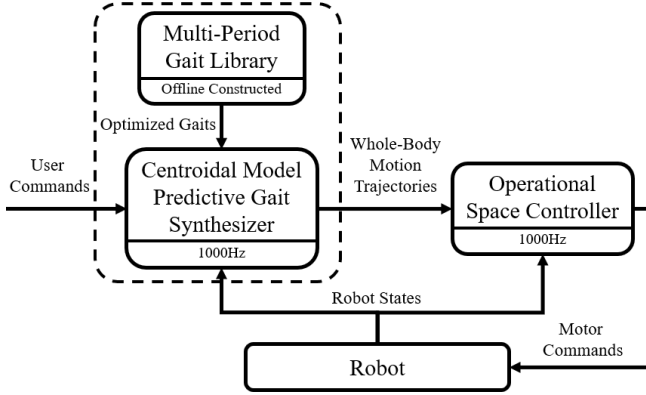


Fig. 1. The overall motion planning and control architecture. The proposed centroidal model predictive gait synthesizer is shown in the dashed box.

for future 2 steps at current time  $t_0$  (assume the right leg is the stance leg at the  $i^{\text{th}}$  step):

$$\begin{aligned}
 & \min_{\varphi(t), T} \int_{t_0}^{2T} \|u_{\varphi(t)} \cdot dq_{\varphi(t)}\|^2 dt \\
 \text{s.t. } & \|\dot{p}_x^+[i+2] - \dot{p}_x^{+*}\| \leq k_1 \|\dot{p}_x^+[i+1] - \dot{p}_x^{+*}\| \\
 & \|\dot{p}_y^+[i+2] - R\dot{p}_y^{+*}\| \leq k_2 \|\dot{p}_y^+[i+1] - L\dot{p}_y^{+*}\| \\
 & \|p_x^+[i+2] - p_x^{+*}\| \leq k_3 \left\| \dot{p}_x^+[i+2] - \begin{bmatrix} \dot{p}_x^{+*} \\ R\dot{p}_y^{+*} \end{bmatrix} \right\| \\
 & \|p_y^+[i+2] - R\dot{p}_y^{+*}\| \leq k_4 \left\| \dot{p}_y^+[i+2] - \begin{bmatrix} \dot{p}_x^{+*} \\ R\dot{p}_y^{+*} \end{bmatrix} \right\| \\
 & \text{Whole-body dynamics satisfied.} \\
 & \text{Whole-body constraints satisfied.}
 \end{aligned} \tag{1}$$

where  $\varphi(t)$  indicates the whole-body motion trajectories,  $T$  is the step period,  $u_{\varphi(t)}$  and  $dq_{\varphi(t)}$  are the joint torques and velocities to achieve  $\varphi(t)$ ,  $p^+[i] = [p_x^+[i]; p_y^+[i]]$  and  $\dot{p}^+[i] = [\dot{p}_x^+[i]; \dot{p}_y^+[i]]$  are the post-impact horizontal CoM position and velocity relative to the stance foot,  $p^{+*} = [p_x^{+*}; Rp_y^{+*}; Lp_y^{+*}]$  and  $\dot{p}^{+*} = [\dot{p}_x^{+*}; R\dot{p}_y^{+*}; L\dot{p}_y^{+*}]$  are the desired values, subscripts  $x, y$  indicate the x/y direction, subscripts  $R, L$  indicate the right/left leg is the stance leg. The constants  $0 < k_1 < 1$ ,  $0 < k_2 < 1$  ensure the contraction of  $\dot{p}^+$ , i.e.,  $\dot{p}_x^+[i+2] \rightarrow \dot{p}_x^{+*}$ ,  $\dot{p}_y^+[i+2] \rightarrow R\dot{p}_y^{+*}$ , and similarly  $\dot{p}_y^+[i+1] \rightarrow L\dot{p}_y^{+*}$ . Then the constants  $0 < k_3 < \infty$ ,  $0 < k_4 < \infty$  ensures  $p_x^+[i+2] \rightarrow p_x^{+*}$  and  $p_y^+[i+2] \rightarrow R\dot{p}_y^{+*}$ . Thus the solution of (1) guarantees the stability of CoM states while satisfying whole-body dynamics and constraints. After each optimization,  $\varphi(t)$  for the next sample time is sent to the controller for tracking.

However, directly solving (1) using whole-body trajectory optimization is extremely time-consuming. In the following sections, we show that our proposed gait synthesizer can provide a feasible solution by combining an offline constructed multi-period gait library and online gait synthesis based on centroidal dynamics. As shown in Fig. 1, this gait synthesizer can run at 1kHz, the same as the OSC. This fast re-planning

greatly increases the robot robustness to disturbances and other environmental uncertainties.

### III. MULTI-PERIOD GAIT LIBRARY

In this section, the multi-period gait library is first constructed through trajectory optimization based on the full dimensional model.

#### A. Hybrid Model of Walking

The walking process is modeled as a hybrid system, including a single support phase and an instantaneous double support phase. Assuming the right leg is the stance leg, the overall hybrid model of walking can be written as:

$$\begin{cases} D(q)\ddot{q} + H(q, \dot{q}) = Bu + J_R(q)^T f_R & (q, \dot{q}) \notin S \\ J_R(q)\ddot{q} + \dot{J}_R(q, \dot{q})\dot{q} = 0 & (q, \dot{q}) \in S \\ \dot{q}^+ = \Delta(q)\dot{q}^- & (q, \dot{q}) \in S \end{cases} \tag{2}$$

where  $S = \{(q, \dot{q}) \in \mathcal{T}\mathcal{Q} \mid p_L^z(q) = 0, \dot{p}_L^z(q, \dot{q}) \leq 0\}$ .

The first two equations in (2) describe the single support phase dynamics. The first equation is the floating base dynamics, where  $q$  is the vector of generalized coordinates including both floating states and joint states,  $D(q)$  is the mass-inertia matrix,  $H(q, \dot{q})$  contains the gravity force and coriolis force,  $u$  is the vector of motor torques,  $f_R$  is the contact wrench.  $B$  is the motor torque distribution matrix,  $J_R(q)$  is the Jacobian matrix of contact points. The second equation is the contact constraint, i.e., the accelerations of the stance foot position and orientation are zero.

The third equation in (2) describes the instantaneous double support phase. When the vertical position of the swing leg  $p_L^z(q)$  decreases to 0, i.e.  $(q, \dot{q}) \in S$ , the robot enters double support phase. Following the rigid impact model hypotheses and development process in [14], the double support phase can be modeled as a discrete map between  $\dot{q}^-$  and  $\dot{q}^+$  (the velocity of the system just before and after impact). Their relationship can be described as:

$$\begin{bmatrix} D(q) & -J_L^T(q) \\ J_L(q) & 0 \end{bmatrix} \begin{bmatrix} \dot{q}^+ \\ f_L \end{bmatrix} = \begin{bmatrix} D(q)\dot{q}^- \\ 0 \end{bmatrix}, \tag{3}$$

where  $f_L := \int_{t_-}^{t_+} \delta f_L(t) dt$  is the integration of the impulsive contact force over the impact instant.  $J_L(q)$  is the Jacobian matrix of the left leg.  $J_L(q)$  has full row rank and  $D(q)$  is positive definite, thus we can invert the left side of (3) and project to get the map between  $\dot{q}^-$  and  $\dot{q}^+$ ,

$$\dot{q}^+ = \Delta(q)\dot{q}^-. \tag{4}$$

Note that if the swing foot impact velocity is 0, the impact will not change the CoM velocity.

#### B. CoM Related Outputs

Each gait in the gait library contains time trajectories of the selected quantities to be controlled, these quantities are termed as 'outputs'. In existing work, joint angles are usually selected as outputs [6], [9] for simplicity. Recently, workspace quantities are also selected as outputs for their physical meanings [15]. While, in this paper, CoM related

quantities are selected as outputs to support the CoM based gait synthesis in Sec. IV.

Specifically, 10 quantities are selected as outputs, they are listed in Tab. I. The CoM x and y positions are not strictly enforced as the stance foot roll and pitch are in fact weakly actuated for limited sole area, these two actuations are used in the controller to regulate the pre-impact COM velocity for active-foot robots. For underactuated bipedal robots, certain quantities are removed from the outputs. For example, for a bipedal robot with fully-passive feet,  $\phi_{foot}$ ,  $\theta_{foot}$  should be removed.

TABLE I  
SELECTED OUTPUTS

Torso roll, pitch and yaw	$\phi_{torso}, \theta_{torso}, \psi_{torso}$
Vertical position of the CoM	$z_{COM}$
Swing foot x and y positions relative to the CoM	$x_{foot}$ $y_{foot}$
Swing foot vertical position	$z_{foot}$
Swing foot roll, pitch and yaw	$\phi_{foot}, \theta_{foot}, \psi_{foot}$

### C. Periodic Gaits Optimization

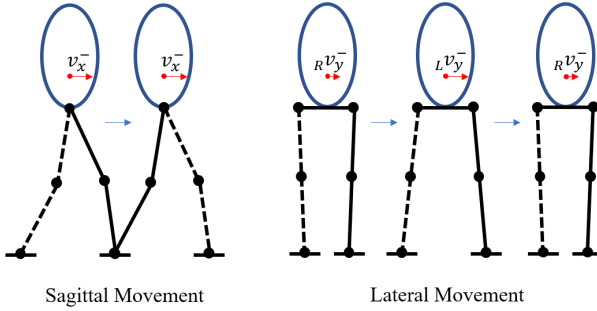


Fig. 2. Difference between sagittal movement and lateral movement.

As shown in Fig. 2, for a periodic gait, the sagittal pre-impact CoM velocity ( $v_x^-$ ) repeats every step, while the lateral pre-impact CoM velocity ( $Rv_y^-$  and  $Lv_y^-$ ) repeats every two steps. Therefore, in order to cover different periodic sagittal and lateral movements, we need to build a gait library with at least four dimensions  $[T, v_x^-, Rv_y^-, Lv_y^-]$ . As the development of trajectory optimization tools such as C-FROST [16], thousands of trajectories can be optimized simultaneously and efficiently, which makes the construction of this gait library possible.

Periodic walking gaits with different sagittal, lateral average velocities and different lateral velocity differences are optimized for multiple periods. The difference of lateral velocity  $\delta v_y^- = Rv_y^- - Lv_y^-$  is also constrained as different combinations of  $Rv_y^-$  and  $Lv_y^-$  can realize the same average lateral velocity. These gait optimization problems are constructed and solved using FROST. Each optimization problem is performed over two steps with the right and left leg being the stance leg successively. The cost function used

in the optimization is the sum square of power:

$$\text{Cost} = \int_0^{2T} \|u \cdot dq\|^2 dt \quad (5)$$

Constraints enforced in the optimization are listed in Tab. II. The swing foot impact velocity is constrained to 0 so that

$$v_x^+ = v_x^-, v_y^+ = v_y^- \quad (6)$$

TABLE II  
CONSTRAINTS USED IN GAIT OPTIMIZATION

Average Sagittal Velocity	$\bar{v}_{x,i}$
Average Lateral Velocity	$\bar{v}_{y,i}$
Difference of Lateral Velocity	$\delta v_y^-$
Period	$T_i$
Friction Cone	$\mu = 0.6$
Mid-step Swing Foot Height	0.07m
Swing Foot Impact Velocity	(0, 0, 0)m/s
Joint Position, Velocity and Torque Limits	Determined by hardware

After these optimizations, we acquire output trajectories for different gaits. All these trajectories are parameterized with Bézier polynomials in terms of the normalized time  $s = t/T$ . For the  $i^{\text{th}}$  output  $h_d^i$ , it can be represented as

$$h_d^i(s) = \sum_{j=0}^M \alpha_j^i \frac{M!}{j!(M-j)!} s^j (1-s)^{M-j}, \quad (7)$$

where  $M$  is the order of the Bézier polynomial. Thus we can use a  $N \times (M+1)$  parameter matrix  $\alpha$  to represent a gait with  $N$  outputs. Additionally, each gait is labeled with its unique  $[T, v_x^-, Rv_y^-, Lv_y^-]$ , i.e.,  $\alpha_{v_x^-, Rv_y^-, Lv_y^-}^T$ .

*Remark 1:* As the lateral movement is comparably slow, it can be approximately modeled as a Linear Inverted Pendulum (LIP). Hence, a simplified gait library with 2 dimensions  $[T, v_x^-]$  can be constructed. The  $y_{foot}$  is calculated online using the LIP model [17]:

$$y_{foot}(T) = \frac{v_y^- - d}{\sigma}, \quad (8)$$

where  $\sigma = \lambda \tanh(\frac{T}{2}\lambda)$ ,  $\lambda = \sqrt{\frac{g}{\bar{z}_{COM}}}$ ,  $d = \frac{\lambda^2 \operatorname{sech}(\frac{T}{2}\lambda)T}{2\sigma} \bar{v}_y$ ,  $T$  is the current period,  $\bar{z}_{COM}$  is the average COM height of current gait. Then  $y_{foot}(T)$  is the swing foot y-axis impact position that can keep the lateral movement in a two-step periodic gait with average lateral velocity  $\bar{v}_y$ .

*Remark 2:* Standing motion can be considered as periodic trajectories with  $\infty$  period. The posture at the beginning of a gait with zero average sagittal and lateral velocity can be directly used for standing.

## IV. CENTROIDAL MODEL PREDICTIVE GAIT SYNTHESIZER

In this section, we propose the MPC style gait synthesizer. It provides a feasible solution of (1) by first predicting the pre-impact CoM states  $\dot{p}^-[i]$ ,  $p^-[i]$  according to current  $\dot{p}$ ,  $p$  and then synthesizing gaits accordingly, as shown in Fig. 3.

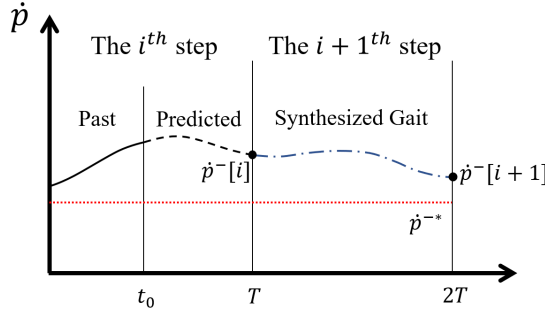


Fig. 3. Our proposed gait synthesizer first predicts  $\dot{p}^-[i]$ ,  $\dot{p}^-[i]$ , then synthesizes a gait such that  $||\dot{p}^-[i+1] - \dot{p}^*|| < ||\dot{p}^-[i] - \dot{p}^*||$ .

#### A. Pre-Impact CoM States Prediction

The pre-impact CoM states  $\dot{p}^-$ ,  $p^-$  are first predicted according to current  $\dot{p}$ ,  $p$ . The centroidal dynamics can be described as:

$$\begin{cases} \ddot{z} = \frac{1}{m} f_z - g \\ \ddot{p} = \frac{1}{m} f_p, \end{cases} \quad (9)$$

where  $z$  is the vertical position of the CoM,  $p$  represents the horizontal position of the CoM, which can be either  $x$  or  $y$  axis position,  $f_p$  and  $f_z$  are ground reaction forces,  $m$  is the total mass,  $g$  is the acceleration of gravity. As the swing and stance legs are generally symmetric and the torso is kept upright, it is reasonable to assume the centroidal angular momentum change rate is 0, i.e.

$$f_p z - f_z p = 0 \quad (10)$$

Combine (9) and (10), we can have

$$\begin{bmatrix} \ddot{z} \\ \ddot{p} \end{bmatrix} = \begin{bmatrix} \frac{1}{m} & -1 \\ p & 0 \end{bmatrix} \begin{bmatrix} f_z \\ g \end{bmatrix}, \quad (11)$$

where  $f_z$  is determined by the PD controller,

$$f_z = (\ddot{z}^* + k_p(z^* - z) + k_d(\dot{z}^* - \dot{z}) + g)m, \quad (12)$$

where  $z^*$ ,  $\dot{z}^*$ ,  $\ddot{z}^*$  are current CoM vertical reference trajectory and its derivatives,  $k_p$  and  $k_d$  are controller parameters. Rearrange (11) and (12), we can have a nonlinear state space model

$$\dot{X} = f_{predict}(X, z^*, \dot{z}^*, \ddot{z}^*, t), \quad (13)$$

where  $X = [z, p, \dot{z}, \dot{p}]^T$ . Given current state  $X(t_0)$ , the pre-impact states can be predicted by numerical integration,

$$X^- = X(T) = \int_{t_0}^T f_{predict}(X, z^*, \dot{z}^*, \ddot{z}^*, t) dt. \quad (14)$$

*Remark:* If  $z^*$  is almost constant during each step,  $\dot{p}^-$  and  $p^-$  can be estimated using the LIP model,

$$\begin{aligned} p^- &= c_1 e^{\lambda(T-t_0)} + c_2 e^{-\lambda(T-t_0)} \\ \dot{p}^- &= \lambda(c_1 e^{\lambda(T-t_0)} - c_2 e^{-\lambda(T-t_0)}), \end{aligned} \quad (15)$$

where  $\lambda = \sqrt{g/z}$ ,  $c_1 = \frac{1}{2}(p + \frac{1}{\lambda}\dot{p})$ ,  $c_2 = \frac{1}{2}(p - \frac{1}{\lambda}\dot{p})$ .

For standing gait, the COM height is constant, the centroidal dynamics can be analysed using the LIP model. Since  $T = \infty$ , we want to predict the COM state in infinite future. If the support region is large enough,  $\dot{p}$  will eventually come to 0, and  $p$  will be at the Capture Point when  $\dot{p} = 0$ , i.e.,

$$\begin{aligned} p^- &= p(\infty) = p + \dot{p}/\sqrt{g/z} \\ \dot{p}^- &= \dot{p}(\infty) = 0 \end{aligned} \quad (16)$$

If  $p(\infty)$  is outside the range of the support region, the robot can not remain standing eventually.

#### B. Gait Synthesis Algorithm

Assume the gait library has  $k$  periods,  $l$  sagittal pre-impact velocities and  $n$  pair of lateral pre-impact velocities. The set of periods is  $S_T = \{T_1, T_2, \dots, T_k\}$  in descending order. The sets of pre-impact velocities are  $S_{v_x^-} = \{v_{x,1}^-, v_{x,2}^-, \dots, v_{x,l}^-\}$ ,  $S_{Rv_y^-} = \{Rv_{y,1}^-, Rv_{y,2}^-, \dots, Rv_{y,n}^-\}$  and  $S_{Lv_y^-} = \{Lv_{y,1}^-, Lv_{y,2}^-, \dots, Lv_{y,n}^-\}$  in which velocities are in ascending order. From now on, the right leg is assumed to be the stance leg, subscripts  $R$  and  $L$  can be swapped for the left leg case. The gait synthesis algorithm is summarized by the pseudo code in Algorithm 1.

---

#### Algorithm 1 Gait Synthesis Algorithm

---

```

1: Input:  $p, \dot{p}, t, i_T^*, \dot{p}^{+*}$ 
2: Output:  $\alpha$ 
3: Initialize:  $Flag = 0$ 
4: for  $i = i_T^*, i_T^* + 1, \dots, k$  do
5:    $T = S_T\{i\}$ 
6:   Predict  $p^-, \dot{p}^-$  with (14) or (16)
7:   if  $(p^-, \dot{p}^-) \in S_{feasible}$  then
8:      $Flag = 1$ 
9:     Break;
10:   end if
11: end for
12: if  $Flag == 1$  then
13:   Gait Interpolation:
14:      $\dot{p}_{y,d}^- = R\dot{p}_y^{+*} + L\dot{p}_y^{+*} - \dot{p}_y^-$ ,
15:      $\alpha_{intp} = G_{intp}(T, \dot{p}_x^-, \dot{p}_y^-, \dot{p}_{y,d}^-)$ .
16:   Gait Modification:
17:      $\alpha = G_{modi}(\alpha_{intp}, \dot{p}_x^-, \dot{p}_y^-, \dot{p}^{+*})$ .
18:   else
19:     Prepare for falling
20:   end if

```

---

In lines 1-3 the input, output and initialization of the algorithm are defined. The input includes current robot states  $p, \dot{p}$ , step time  $t$ , the index  $i_T^*$  of the desired period  $T^*$  ( $T^* = S_T\{i_T^*\}$ ) and the desired post-impact velocities  $\dot{p}^{+*}$ . The output is the synthesized gait parameter  $\alpha$ . The variable  $Flag$  is the flag for finding a feasible  $\alpha$ .

In lines 4-11 the gait period is first determined by traversing the period set  $S_T$  from the  $i_T^*$ -th element, until a feasible  $T$  is found. A  $T$  is feasible if the predicted  $(p^-, \dot{p}^-)$  with this  $T$  is in  $S_{\text{feasible}}$ . The feasible set  $S_{\text{feasible}}$  is defined as

$$S_{\text{feasible}} = \{(p^-, \dot{p}^-) | p^- \in S_{\text{CoM}}, g_{\text{foot}}(T, \dot{p}^-) \in S_{\text{foot}}\}, \quad (17)$$

where  $g_{\text{foot}}(T, \dot{p}^-)$  calculates the predicted pre-impact swing foot position,  $S_{\text{CoM}}$  and  $S_{\text{foot}}$  are feasible regions of CoM position and swing foot position, they are designed to satisfy the workspace limit and avoid foot collision. If the predicted  $(p^-, \dot{p}^-)$  with current  $T$  is not feasible, a smaller  $T$  is tested as decreasing step time enlarges the feasible region. Note that this procedure is executed at each sample time, thus  $T$  may be changed anytime during a step.

In line 13 the gait parameter  $\alpha$  is synthesized if a feasible period  $T$  is found. First, the gait library is interpolated by tri-linear interpolation:

$$\begin{aligned} G_{\text{intp}}(T, \dot{p}_x^-, \dot{p}_y^-, \dot{p}_{y,d}^-) := & \alpha_{v_x^-, v_{x,i+1}, Rv_{y,j+1}, Lv_{y,k+1}}^T \xi_1 \xi_2 \xi_3 \\ & + \alpha_{v_x^-, v_{x,i}, Rv_{y,j}, Lv_{y,k}}^T (1 - \xi_1)(1 - \xi_2)(1 - \xi_3) \\ & + \alpha_{v_x^-, v_{x,i+1}, Rv_{y,j}, Lv_{y,k}}^T \xi_1 (1 - \xi_2)(1 - \xi_3) \\ & + \alpha_{v_x^-, v_{x,i}, Rv_{y,j+1}, Lv_{y,k}}^T (1 - \xi_1)\xi_2(1 - \xi_3) \\ & + \alpha_{v_x^-, v_{x,i}, Rv_{y,j}, Lv_{y,k+1}}^T (1 - \xi_1)(1 - \xi_2)\xi_3 \\ & + \alpha_{v_x^-, v_{x,i+1}, Rv_{y,j}, Lv_{y,k+1}}^T \xi_1 (1 - \xi_2)\xi_3 \\ & + \alpha_{v_x^-, v_{x,i+1}, Rv_{y,j+1}, Lv_{y,k}}^T \xi_1 \xi_2 (1 - \xi_3) \\ & + \alpha_{v_x^-, v_{x,i}, Rv_{y,j+1}, Lv_{y,k}}^T (1 - \xi_1)\xi_2\xi_3, \end{aligned} \quad (18)$$

if  $v_{x,i}^- \leq \dot{p}_x^- \leq v_{x,i+1}^-, Rv_{y,j}^- \leq \dot{p}_y^- \leq Rv_{y,j+1}^-, Lv_{y,k}^- \leq \dot{p}_{y,d}^- \leq Lv_{y,k+1}^-$ , where  $\dot{p}_{y,d}^- = R\dot{p}_y^{+*} + L\dot{p}_y^{+*} - \dot{p}_y^-$ ,  $\xi_1 = \frac{\dot{p}_x^- - v_{x,i}^-}{v_{x,i+1}^- - v_{x,i}^-}$ ,  $\xi_2 = \frac{\dot{p}_y^- - Rv_{y,j}^-}{Rv_{y,j+1}^- - Rv_{y,j}^-}$ ,  $\xi_3 = \frac{\dot{p}_{y,d}^- - Lv_{y,k}^-}{Lv_{y,k+1}^- - Lv_{y,k}^-}$ .

In line 14 the footstrike locations are adjusted to regulate  $\dot{p}^-$  by modifying the last parameter of the 4<sup>th</sup> and 5<sup>th</sup> output ( $x_{\text{foot}}$  and  $y_{\text{foot}}$ ) of this gait, with a discrete P controller.

$$\begin{aligned} G_{\text{modi}}(\alpha_{\text{intp}}, \dot{p}_x^-, \dot{p}_y^-, \dot{p}^{+*}) := & \left\{ \begin{array}{l} \alpha = \alpha_{\text{intp}}; \\ \alpha(4, M+1) = \alpha(4, M+1) + k_x(\dot{p}_x^- - \dot{p}_x^{+*}); \\ \alpha(5, M+1) = \alpha(5, M+1) - k_y(\dot{p}_y^- - L\dot{p}_y^{+*}); \end{array} \right\} \end{aligned} \quad (19)$$

This regulator-type controller has been successfully implemented in [9], [17], [18].

In lines 15-17 the robot prepares for falling if no feasible gait is found.

### C. Stability Analysis

In this section, we present the proof for stability of  $p$  and  $\dot{p}$  by showing that the generated gait of our gait synthesizer is a feasible solution of (1). First, some definitions are given. The velocity range of the gait library is

$$S_v = \{(v_x^-, Rv_y^-, Lv_y^-) | v_{x,1}^- \leq v_x^- \leq v_{x,l}^-, Rv_{y,1}^- \leq Rv_y^- \leq Rv_{y,n}^-, Lv_{y,1}^- \leq Lv_y^- \leq Lv_{y,n}^-\}. \quad (20)$$

The poincaré map of the pre-impact CoM velocities between steps are defined as  $P_{\text{map}}$ , i.e.,

$$P_{\text{map}}(\alpha_i, \dot{p}_x^-[i], \dot{p}_y^-[i]) := [\dot{p}_x^-[i+1], \dot{p}_y^-[i+1]], \quad (21)$$

where  $\alpha_i$  is the gait parameter implemented for the  $i^{\text{th}}$  step.

Then two assumptions are given about gait interpolation and modification.

**Assumption 1.** For any  $[v_x^-, Rv_y^-, Lv_y^-] \in S_v$ , implementing the interpolated gait  $\alpha_{\text{intp}} = G_{\text{intp}}(T, v_x^-, Rv_y^-, Lv_y^-)$  will give us:

$$P_{\text{map}}(\alpha_{\text{intp}}, v_x^-, Rv_y^-) = [v_x^-, Lv_y^-]. \quad (22)$$

**Assumption 2.** There exist  $\delta_x, \delta_y \in \mathbb{R}^-$  such that, for any  $[v_x^-, Rv_y^-, Lv_y^-] \in S_v$  and  $\alpha_{\text{intp}} = G_{\text{intp}}(T, v_x^-, Rv_y^-, Lv_y^-)$ , the states of the next step  $[\dot{p}_x^-[i+1], \dot{p}_y^-[i+1]] = P_{\text{map}}(\alpha_{\text{intp}}, v_x^-, Rv_y^-)$  satisfy:

$$\begin{aligned} \delta_x & \leq \frac{\partial \dot{p}_x^-[i+1]}{\partial \alpha(4, M+1)} \Big|_{[\alpha_{\text{intp}}, v_x^-, Rv_y^-]} < 0, \\ \delta_y & \leq \frac{\partial \dot{p}_y^-[i+1]}{\partial \alpha(5, M+1)} \Big|_{[\alpha_{\text{intp}}, v_x^-, Rv_y^-]} < 0. \end{aligned} \quad (23)$$

■

The first assumption is based on the fact that each gait  $\alpha_{v_x^-, Rv_y^-, Lv_y^-}^T$  in the gait library satisfies

$$P_{\text{map}}(\alpha_{v_x^-, Rv_y^-, Lv_y^-}^T, v_x^-, Rv_y^-) = [v_x^-, Lv_y^-], \quad (24)$$

thus the interpolated gait is assumed to satisfy (22) at the in-between velocities. If we build a gait library with infinite small grid size, this assumption intuitively holds.

The second assumption indicates that finite adjustment of the footstrike location makes finite change of  $\dot{p}^-$  in the opposite direction. This can be case-checked for any  $[v_x^-, Rv_y^-, Lv_y^-] \in S_v$  through numerical simulation.

**Proposition 1.** Each element  $g_{\text{intp}}(T, V)$  of  $G_{\text{intp}}(T, V)$  is Lipschitz continuous for  $V \in S_v$ , with  $K$  being the largest Lipschitz constant, i.e., for all  $V_1, V_2 \in S_v$ ,

$$\|g_{\text{intp}}(T, V_1) - g_{\text{intp}}(T, V_2)\| \leq K\|V_1 - V_2\|. \quad (25)$$

The proof is presented in the appendix. ■

**Theorem 1.** The generated gait of our gait synthesis algorithm is a feasible solution of (1), if

$$0 < k_x < -\frac{2}{\delta_x}, 0 < k_y < -\frac{2}{\delta_y}. \quad (26)$$

*Proof:* (Assume the right leg is the stance leg for step  $i$ )

We prove for the lateral direction first since it is more complex, the proof for the sagittal direction is similar.

First, we show that

$$\|\dot{p}_y^+[i+2] - R\dot{p}_y^{+*}\| \leq k_2\|\dot{p}_y^+[i+1] - L\dot{p}_y^{+*}\| \quad (27)$$

According to (18),(19),(22):

$$\dot{p}_y^-[i+1] = \dot{p}_y^-[i] - \frac{\partial \dot{p}_y^-[i+1]}{\partial \alpha(5, M+1)} k_y(\dot{p}_y^-[i] - L\dot{p}_y^{+*}), \quad (28)$$

where  $\dot{p}_{y,d}^-[i] = {}_R\dot{p}_y^{+*} + {}_L\dot{p}_y^{+*} - \dot{p}_y^-[i]$ . Furthermore, (6) indicates that  $\dot{p}^+[i+2] = \dot{p}^-[i+1]$ . Thus

$$\begin{aligned} \|\dot{p}_y^+[i+2] - {}_R\dot{p}_y^{+*}\| &= \|\dot{p}_y^-[i+1] - {}_R\dot{p}_y^{+*}\| \\ &= \|(1 + \frac{\partial \dot{p}_y^-[i+1]}{\partial \alpha(5,M+1)} k_y)({}_L\dot{p}_y^{+*} - \dot{p}_y^-[i])\| \\ &= \left\|1 + \frac{\partial \dot{p}_y^-[i+1]}{\partial \alpha(5,M+1)} k_y\right\| \|\dot{p}_y^+[i+1] - {}_L\dot{p}_y^{+*}\| \end{aligned} \quad (29)$$

According to (23), (26),  $\left\|1 + \frac{\partial \dot{p}_y^-[i+1]}{\partial \alpha(5,M+1)} k_y\right\| \leq \left\|1 + \delta_y k_y\right\| < 1$ , hence (27) is proved, with  $k_2 = \left\|1 + \delta_y k_y\right\|$ .

Next we show that

$$\|\dot{p}_y^+[i+2] - {}_R\dot{p}_y^{+*}\| \leq k_4 \left\| \dot{p}^+[i+2] - \begin{bmatrix} \dot{p}_x^{+*} \\ {}_R\dot{p}_y^{+*} \end{bmatrix} \right\|. \quad (30)$$

The post-impact CoM position equals to the negative value of the pre-impact swing foot position, i.e.,  $p^+[i+1] = -p_{foot}^-[i]$ . Pre-impact swing foot position is part of the output of  $G_{intp}$ , noted as  $g_{foot}$ . For the desired periodic gait,  $p^{+*}$  and  $\dot{p}^{+*}$  should satisfy

$${}_R\dot{p}_y^{+*} = -g_{foot}^y(T, \dot{p}_x^{+*}, {}_R\dot{p}_y^{+*}, {}_L\dot{p}_y^{+*}). \quad (31)$$

Consider the  $i+1^{\text{th}}$  step, according to (18), (19),

$$\begin{aligned} p_y^+[i+2] &= -g_{foot}^y(T, \dot{p}_x^-[i+1], \dot{p}_y^-[i+1], \dot{p}_{y,d}^-[i+1]) \\ &+ k_y(\dot{p}_y^-[i+1] - {}_R\dot{p}_y^{+*}) \end{aligned} \quad (32)$$

Thus,

$$\begin{aligned} \|\dot{p}_y^+[i+2] - {}_R\dot{p}_y^{+*}\| &= \|g_{foot}^y(T, \dot{p}_{aug}^-[i+1]) - \\ &k_y(\dot{p}_y^-[i+1] - {}_R\dot{p}_y^{+*}) - g_{foot}^y(T, \dot{p}^{+*})\| \\ &\leq \|g_{foot}^y(T, \dot{p}_{aug}^-[i+1]) - g_{foot}^y(T, \dot{p}^{+*})\| + \\ &k_y \|\dot{p}_y^-[i+1] - {}_R\dot{p}_y^{+*}\| \end{aligned} \quad (33)$$

where  $\dot{p}_{aug}^-[i+1] = [\dot{p}_x^-[i+1]; \dot{p}_y^-[i+1]; \dot{p}_{y,d}^-[i+1]]$ .

Then, according to (25) and (6)

$$\begin{aligned} \|\dot{p}_y^+[i+2] - {}_R\dot{p}_y^{+*}\| &\leq K \|\dot{p}_{aug}^-[i+1] - \dot{p}^{+*}\| + k_y \|\dot{p}_y^-[i+1] - {}_R\dot{p}_y^{+*}\| \\ &= K \left\| \begin{bmatrix} \dot{p}_x^+[i+2] - \dot{p}_x^{+*} \\ \dot{p}_y^+[i+2] - {}_R\dot{p}_y^{+*} \\ {}_R\dot{p}_y^{+*} - \dot{p}_y^+[i+2] \end{bmatrix} \right\| + k_y \|\dot{p}_y^+[i+2] - {}_R\dot{p}_y^{+*}\| \\ &\leq (\sqrt{2}K + k_y) \left\| \dot{p}^+[i+2] - \begin{bmatrix} \dot{p}_x^{+*} \\ {}_R\dot{p}_y^{+*} \end{bmatrix} \right\|. \end{aligned} \quad (34)$$

Thus (30) is proved with  $k_4 = \sqrt{2}K + k_y$ .

Similarly, we can prove for the sagittal direction that

$$\|\dot{p}_x^+[i+2] - \dot{p}_x^{+*}\| \leq k_1 \|\dot{p}^+[i+1] - \dot{p}_x^{+*}\|, \quad (35)$$

$$\|\dot{p}_x^+[i+2] - \dot{p}_x^{+*}\| \leq k_3 \left\| \dot{p}^+[i+2] - \begin{bmatrix} \dot{p}_x^{+*} \\ {}_R\dot{p}_y^{+*} \end{bmatrix} \right\|. \quad (36)$$

Additionally, the generated gait is synthesized from gaits optimized based on the full dimensional model with cost function (5), hence satisfies the whole-body dynamics and constraints. Thus the generated gait of our gait synthesis algorithm is a feasible sub-optimal solution of (1). ■

## V. IMPLEMENTATION RESULTS

This section presents simulation and experimental results of the proposed gait synthesizer. An 8-DoF bipedal robot is used in the simulation. As shown in Fig. 4, the robot has four actuators each leg, they are for hip abduction, hip flexion, knee and ankle respectively. A physical robot is built according to this model with passive ankles, whose actuators are to be added in the future.

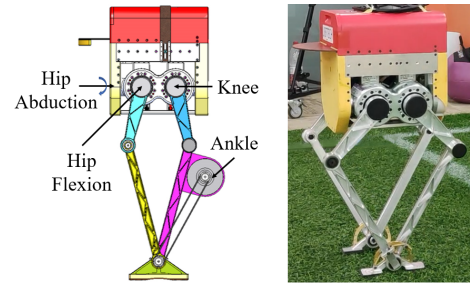


Fig. 4. Bipedal robots for simulation and experiment.

### A. Simulation Results

We first show simulation results on the 8-DoF robot model. The gait library is constructed with 3 periods  $\{\infty, 0.35, 0.2\}$  and 8 sagittal average velocities  $\{-0.5, -0.3, -0.15, 0, 0.15, 0.3, 0.5, 0.7\}$ , the periodic gait for the lateral direction is calculated using the LIP model. The controller used in the simulation is a QP-based operational space controller, similar to the one used in [19]. The gait modification parameters are  $k_x = 0.08$ ,  $k_y = 0.095$ , same for all simulations.

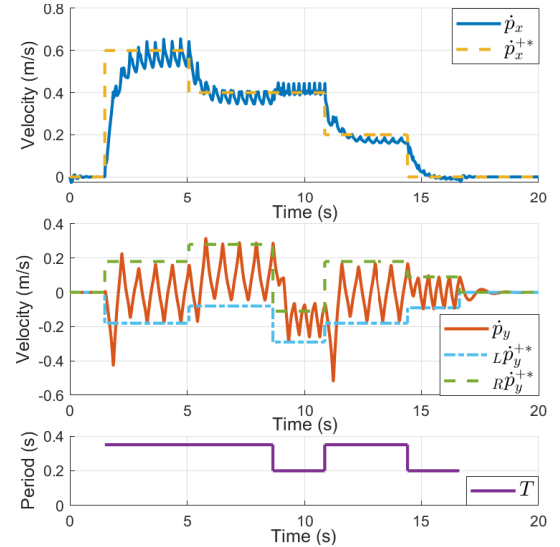


Fig. 5. The first two figures show the velocities of the robot walking and standing following the user command  $T, \dot{p}_x^{+*}, {}_R\dot{p}_y^{+*}, {}_L\dot{p}_y^{+*}$ . The third figure shows the gait period, for the missed part  $T = \infty$ , the robot is standing.

The first simulation is walking and standing following the user command. As shown in Fig. 5, the third figure shows

the desired  $T$ , which starts as  $\infty$ , then varies among 0.2s and 0.35s, and finally returns to  $\infty$ . Thus, the robot started from standing, then transitioned to walking following the desired velocity commands, finally returned to standing. We can see that the robot followed the desired  $\dot{p}_x^{+*}, R\dot{p}_y^{+*}, L\dot{p}_y^{+*}$  very responsively and accurately.

TABLE III  
THE TIME AND MAGNITUDE OF IMPULSES.

Time	4s	8s	12s	16s	20s	24s
Sagittal	5Ns	7Ns	0	0	9Ns	9Ns
Lateral	0	0	2Ns	4Ns	-6Ns	6Ns

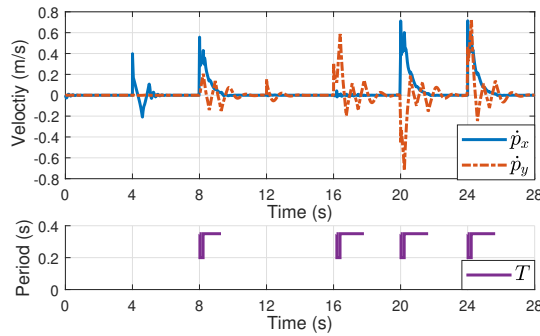


Fig. 6. The first figure shows the velocities of the robot under impulse disturbances. The second figure shows the gait period, for the missed part  $T = \infty$ , the robot is standing.

The second simulation is push-recovery test. The robot started from standing. Six impulses with different magnitudes were applied to the robot in the sagittal and lateral direction. The magnitude and applied time of these impulses are shown in Tab. III. As shown in Fig. 6, for the first and third impulse, the robot recovered to steady state purely by the standing controller. While for other cases, the robot detected that it can not remain standing and automatically took steps with appropriate periods and then returned to standing. The robot recovered from instant velocity change up to 0.7m/s in the sagittal direction and 0.5m/s in the lateral direction.

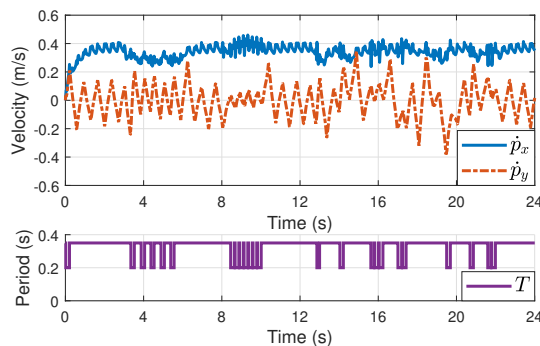


Fig. 7. The first figure shows the velocities of the robot walking over the uneven terrain blindly. The second figure shows the period of gait.

The third simulation is rough terrain test. As shown in

Fig. 8, the robot blindly walked over a rough terrain with 15 degree slopes, 5cm stairs and 2-5cm boards. The desired speed is 0.4m/s and the nominal period is 0.35s. The velocity and gait period are shown in Fig. 7, we can see that the robot successfully passed this terrain with small velocity variation.

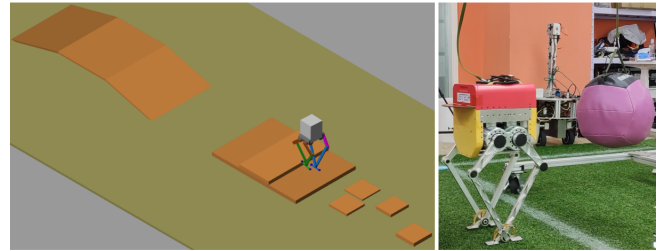


Fig. 8. The left picture shows the rough terrain with 15 degrees slopes, 5cm stairs and 2-5cm boards. The right picture shows the robot is hit by a 5kg wall ball while stepping in place.

### B. Experimental Results

Finally we apply the proposed gait synthesizer to the physical robot in Fig. 4. The same gait library and controller were used for experiments, and the robot achieved stable walking with maximal speed 0.7m/s. The result of push-recovery experiment is presented here. As shown in Fig. 8, the robot was hit by a 5kg wall ball in the sagittal direction for 6 times while stepping in place. The velocity and gait period are shown in Fig. 9, we can see the robot recovered from instant velocity change up to 0.8m/s.

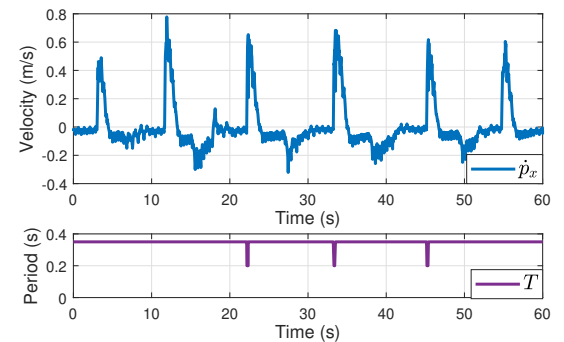


Fig. 9. The first figure shows the sagittal velocity of the robot during the push recovery experiment. The second figure shows the gait period.

## VI. CONCLUSION

The results in this paper provide a method towards full dimensional model based real-time motion planning for bipedal locomotion with theoretical stability guarantee. The planning of whole-body motion and step time is constructed as an MPC problem, in which a sequence of optimization problems need to be solved online. We showed that our proposed gait synthesizer can solve these optimization problems quickly online and thus guarantees the feasibility and stability of the full dimensional robot. With this proposed method, robots achieved flexible transitions between standing and

walking with different periods/speeds according to the user command and robust locomotion under large disturbances or environmental uncertainties.

This paper also provides a perspective that offline computation of whole-body dynamics and online computation of concentrated dynamics (such as the centroidal dynamics) can be combined to achieve real-time whole-body motion planning.

Future work will be extending current work to locomotion planning with terrain knowledge. While robots can accommodate simple rough terrains blindly with current method, passing more complex terrains still needs a perceptive planner. Exploring more intelligent methods of combining whole-body dynamics and centroidal dynamics for motion planning is also a future direction.

## ACKNOWLEDGMENT

This work was supported by UBTECH Robotics.

## APPENDIX

### Proof of Proposition 1:

$S_v$  is split into  $(l-1) \times (n-1) \times (n-1)$  subsets with each subset defined as

$$\begin{aligned} S_v^{i,j,k} = \{V = [v_1, v_2, v_3] \mid & v_{x,i}^- \leq v_1 \leq v_{x,i+1}^-, \\ & Rv_{y,j}^- \leq v_2 \leq Rv_{y,j+1}^-, Lv_{y,k}^- \leq v_3 \leq Lv_{y,k+1}^-\}. \end{aligned} \quad (37)$$

In each subset, every element of  $G_{intp}(T, V)$  can be written as a cubic function according to (18)

$$\begin{aligned} g_{intp}(T, V) = & a_1 v_1 v_2 v_3 + a_2 v_1 v_2 + a_3 v_1 v_3 \\ & + a_4 v_2 v_3 + a_5 v_1 + a_6 v_2 + a_6 v_3 + a_7, \end{aligned} \quad (38)$$

where  $a_1$  to  $a_7$  are constants. It's easy to show that  $g_{intp}(T, V)$  is Lipschitz continuous in each subset.

Additionally,  $S_v$  is convex according to (20), thus for  $V_1, V_2 \in S_v$ , the line connecting  $V_1, V_2$  passes finite number of subsets of  $S_v$  and intersects the boundaries of subsets at  $o$  points  $(V_{m,1}, V_{m,2}, \dots, V_{m,o})$  and

$$\begin{aligned} \|V_1 - V_2\| = & \|V_1 - V_{m,1}\| + \|V_{m,1} - V_{m,2}\| + \\ & \dots + \|V_{m,o-1} - V_{m,o}\| + \|V_{m,o} - V_2\| \end{aligned} \quad (39)$$

Let  $K$  be the largest Lipschitz constant of all subsets for all  $g_{intp}$ . As  $g_{intp}(T, V)$  is continuous at the boundaries, we can have

$$\begin{aligned} \|g_{intp}(T, V_1) - g_{intp}(T, V_2)\| &= \|g_{intp}(T, V_1) - \\ & g_{intp}(T, V_{m,1}) + \dots + g_{intp}(T, V_{m,o}) - g_{intp}(T, V_2)\| \\ &\leq \|g_{intp}(T, V_1) - g_{intp}(T, V_{m,1})\| + \dots + \\ & \|g_{intp}(T, V_{m,o}) - g_{intp}(T, V_2)\| \\ &\leq K\|V_1 - V_{m,1}\| + \dots + K\|V_{m,o} - V_2\|. \end{aligned} \quad (40)$$

Then according to (39), we can have

$$\|g_{intp}(T, V_1) - g_{intp}(T, V_2)\| \leq K\|V_1 - V_2\|,$$

which completes the proof.

## REFERENCES

- [1] M. H. Raibert, *Legged robots that balance*. MIT press, 1986.
- [2] S. Kajita, H. Hirukawa, K. Harada, and K. Yokoi, *Introduction to humanoid robotics*. Springer, 2014, vol. 101.
- [3] J. Englsberger, C. Ott, and A. Albu-Schäffer, "Three-dimensional bipedal walking control based on divergent component of motion," *Ieee transactions on robotics*, vol. 31, no. 2, pp. 355–368, 2015.
- [4] H. Dai, A. Valenzuela, and R. Tedrake, "Whole-body motion planning with centroidal dynamics and full kinematics," in *2014 IEEE-RAS International Conference on Humanoid Robots*. IEEE, 2014, pp. 295–302.
- [5] M. Posa, S. Kuindersma, and R. Tedrake, "Optimization and stabilization of trajectories for constrained dynamical systems," in *2016 IEEE International Conference on Robotics and Automation (ICRA)*. IEEE, 2016, pp. 1366–1373.
- [6] E. R. Westervelt, J. W. Grizzle, and C. C. De Wit, "Switching and pi control of walking motions of planar biped walkers," *IEEE Transactions on Automatic Control*, vol. 48, no. 2, pp. 308–312, 2003.
- [7] M. J. Powell, A. Hereid, and A. D. Ames, "Speed regulation in 3d robotic walking through motion transitions between human-inspired partial hybrid zero dynamics," in *2013 IEEE international conference on robotics and automation*. IEEE, 2013, pp. 4803–4810.
- [8] V. Murali, A. D. Ames, and E. I. Verriest, "Optimal walking speed transitions for fully actuated bipedal robots," in *2019 IEEE 58th Conference on Decision and Control (CDC)*. IEEE, 2019, pp. 6295–6300.
- [9] X. Da, O. Harib, R. Hartley, B. Griffin, and J. W. Grizzle, "From 2d design of underactuated bipedal gaits to 3d implementation: Walking with speed tracking," *IEEE Access*, vol. 4, pp. 3469–3478, 2016.
- [10] S. Feng, "Online hierarchical optimization for humanoid control," Ph.D. dissertation, Carnegie Mellon University, 2016.
- [11] H. Wang and M. Zhao, "A robust biped gait controller using step timing optimization with fixed footprint constraints," in *2017 IEEE International Conference on Robotics and Biomimetics (ROBIO)*. IEEE, 2017, pp. 1787–1792.
- [12] M. Khadiv, A. Herzog, S. A. A. Moosavian, and L. Righetti, "Walking control based on step timing adaptation," *IEEE Transactions on Robotics*, 2020.
- [13] T. Koolen, T. De Boer, J. Rebula, A. Goswami, and J. Pratt, "Capturability-based analysis and control of legged locomotion, part 1: Theory and application to three simple gait models," *The international journal of robotics research*, vol. 31, no. 9, pp. 1094–1113, 2012.
- [14] E. R. Westervelt, J. W. Grizzle, C. Chevallereau, J. H. Choi, and B. Morris, *Feedback control of dynamic bipedal robot locomotion*. CRC press, 2018.
- [15] Y. Gong, R. Hartley, X. Da, A. Hereid, O. Harib, J.-K. Huang, and J. Grizzle, "Feedback control of a cassie bipedal robot: Walking, standing, and riding a segway," in *2019 American Control Conference (ACC)*. IEEE, 2019, pp. 4559–4566.
- [16] A. Hereid, O. Harib, R. Hartley, Y. Gong, and J. W. Grizzle, "Rapid trajectory optimization using c-frost with illustration on a cassie-series dynamic walking biped," in *2019 IEEE/RSJ International Conference on Intelligent Robots and Systems (IROS)*. IEEE, 2019, pp. 4722–4729.
- [17] X. Xiong and A. D. Ames, "Orbit characterization, stabilization and composition on 3d underactuated bipedal walking via hybrid passive linear inverted pendulum model," in *2019 IEEE/RSJ International Conference on Intelligent Robots and Systems (IROS)*. IEEE, 2019, pp. 4644–4651.
- [18] S. Rezazadeh, C. Hubicki, M. Jones, A. Peekema, J. Van Why, A. Abate, and J. Hurst, "Spring-mass walking with atrias in 3d: Robust gait control spanning zero to 4.3 kph on a heavily underactuated bipedal robot," in *ASME 2015 dynamic systems and control conference*. American Society of Mechanical Engineers Digital Collection, 2015.
- [19] T. Apgar, P. Clary, K. Green, A. Fern, and J. W. Hurst, "Fast online trajectory optimization for the bipedal robot cassie," in *Robotics: Science and Systems*, vol. 101, 2018, p. 14.